

THE AFTERGLOWS OF ULTRALUMINOUS QUASARS

JIAN-MIN WANG¹, YE-FEI YUAN² AND LUIS C. HO³

Accepted by The Astrophysical Journal Letters

ABSTRACT

Quasars represent a brief phase in the life-cycle of most massive galaxies, but the evolutionary connection between central black holes and their host galaxies remains unclear. While quasars are active and shining brighter than the Compton-limit luminosity, their radiation heats the surrounding medium to the Compton temperature, forming Compton spheres extending to the Strömgen radius of Fe²⁶⁺/He²⁺. After the quasars shut off, their “afterglow” can be detected through three signatures: (1) an extended X-ray envelope, with a characteristic temperature of $\sim 3 \times 10^7$ K; (2) Ly α and Ly β lines and the K-edge of Fe²⁶⁺; and (3) nebulosity from hydrogen and helium recombination emission lines. We discuss the possibility of detecting these signatures using *Chandra*, the planned *XEUS* mission, and ground-based optical telescopes. The luminosity and size of quasar afterglows can be used to constrain the lifetime of quasars.

Subject headings: black hole physics — cosmology: theory — galaxies: formation — quasar: general

1. INTRODUCTION

The neutral hydrogen bounded by dark matter halos at high redshift has detectable extended Ly α “fuzz” powered by photoionization from central quasars (Haiman & Rees 2001). The detection of this signal may impose strong constraints on quasar formation during galaxy assembly. The lifetime of quasars remains uncertain, but they are generally thought to be short-lived, with estimated ages of $\sim 10^7$ to 10^9 years (Jakobsen et al. 2003; Martini & Schneider 2003). Detecting the infalling gas, heated by the quasar, as Ly α fuzz can help to constrain the quasar’s lifetime. If undetected, it may imply that quasar activity only appears when the gas has settled into a thin disk or has already been consumed mostly by star formation. The preliminary evidence for extended Ly α emission in radio-quiet quasars already suggests that quasar activity influences galaxy assembly (Bergeron et al. 1999; Fardal et al. 2001; Bunker et al. 2003). The spectrum of the quasar Q1205–30 unambiguously shows an extended hydrogen Ly α glow formed by gas falling into the ionizing cone of the quasar (Weidinger et al. 2004).

What is the physical appearance of a quasar turning *off* within an assembling galaxy? This Letter investigates the afterglow properties of ultraluminous, radio-quiet quasars.

2. COMPTON SPHERE AND COMPTON LIMIT

While the quasar is active, it provides a source of energy to heat infalling material (Binney & Tabor 1995; Ciotti & Ostriker 2001; Brighenti & Mathews 2002). Hot gas in elliptical galaxies has been extensively studied for three decades since *Einstein*, but the physics of its origin and evolution still are not completely understood (see the review by Mathews & Brighenti 2003). It has been realized that gas infalling into the dark matter halo of a nascent galaxy (Fall & Rees 1985) undergoes thermal instability and forms a two-phase medium that would exhibit very faint emission features (Haiman, Spaans & Quataert 2000). In this stage, pressure balance holds between the cold ($T_c \approx 10^4$ K) and hot ($T_h \approx 10^6$ K) medium. The clumping factor of the two-phase medium is $\mathcal{C} = \langle n_b^2 \rangle / \langle n_b \rangle^2 = (T_h/T_c)^2 \approx$

10^4 , where n_b is the baryon number density. The irradiation by the quasar light greatly changes the two-phase structure of the infalling gas. We assume the abundance of hydrogen, helium and iron to be $\mathcal{A}_H = 0.7$, $\mathcal{A}_{He} = 0.3$ and $\mathcal{A}_{Fe} = 5.0 \times 10^{-5}$, respectively. The thermal state of the photoionized gas is determined by the ionization parameter, defined by

$$\Xi = \frac{F}{cnkT}, \quad (1)$$

where n and T are the number density and temperature of the gas and F is the flux of the ionizing source (Krolik, McKee & Tarter 1981). Compton heating and cooling balance at a temperature of $T_C = \tilde{\epsilon}/4k$, where $\tilde{\epsilon}$ is the mean energy of the ionizing source and k is Boltzmann’s constant. For a typical quasar spectrum (Elvis et al. 1994), the mean photon energy is $\tilde{\epsilon} \approx 10$ keV. The gas will be heated to $T_C \approx 3.0 \times 10^7$ K (see the detailed calculation of Sazonov et al. 2004), which is one order of magnitude hotter than the typical virial temperature of 0.15 keV for the hot gas (Fall & Rees 1985). When the ionization parameter of the ionized gas reaches

$$\Xi \geq \Xi_C = 6.1 \tilde{\epsilon}_1^{-3/2}, \quad (2)$$

where $\tilde{\epsilon}_1 = \tilde{\epsilon}/10$ keV, the gas will be fully heated to the Compton temperature (Krolik, McKee & Tarter 1981). The timescale of Compton heating is given by $t_C^{\text{heat}} = 3m_e c^2 k T_C / 8\sigma_T \tilde{\epsilon} F$, where m_e is the electron mass and σ_T is the Thomson scattering cross section. This timescale is derived by dividing the number of scatterings needed to reach the Compton temperature by the scattering rate. We assume a quasar lifetime of $t_Q = \tau_Q t_{\text{Salp}}$, with $t_{\text{Salp}} = 4.6 \times 10^8$ yr being the Salpeter timescale (Salpeter 1964). Setting $t_C^{\text{heat}} = t_Q$, with $L_{46} = L/10^{46}$ erg s⁻¹, we have the Compton radius

$$R_C = 3.2 L_{46}^{1/2} \tau_Q^{1/2} \text{ kpc}, \quad (3)$$

which, along with the condition $\Xi = \Xi_C$, gives the Compton density

$$n_C = 1.1 \times 10^{-2} \tau_Q^{-1} \tilde{\epsilon}_1^{1/2} \text{ cm}^{-3}. \quad (4)$$

¹Laboratory for High Energy Astrophysics, Institute of High Energy Physics, Chinese Academy of Sciences, Beijing 100039, China; wangjm@mail.ihep.ac.cn

²Center for Astrophysics, University of Science and Technology of China, Hefei 230026, China; yfyuan@ustc.edu.cn

³The Observatories of the Carnegie Institution of Washington, 813 Santa Barbara Street, Pasadena, CA 91101, USA; lho@ociw.edu

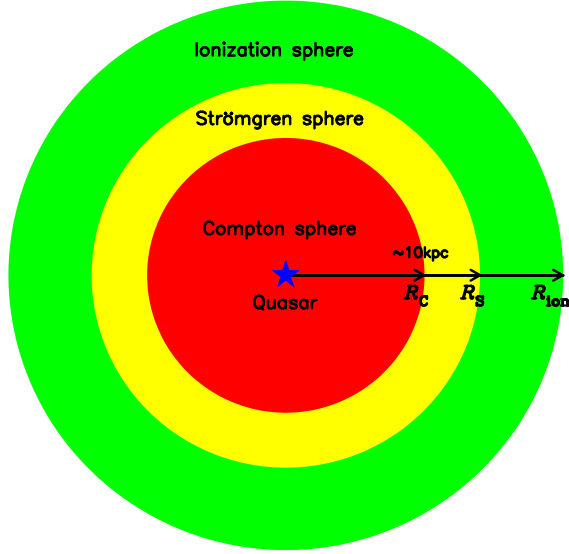


FIG. 1.— Illustration of the afterglow from an ultraluminous quasar. The Compton radius, R_C , extends to the Strömgen radius, R_S , during the quasar’s lifetime when its luminosity exceeds the Compton limit luminosity. The afterglow arises from the Compton sphere after the quasar is extinct.

The Compton radius depicts the size of the region in which the gas is heated by the quasar to the Compton temperature during the timescale t_Q . The Compton density is the maximum density allowed within R_C by Compton heating during the lifetime of the quasar. It is interesting to note that n_C is independent of the quasar luminosity. Beyond R_C , the gas has an ionization parameter of $\Xi < \Xi_C$ and hence is in a two-phase state. For a medium with a density lower than n_C , the size of the region with $\Xi > \Xi_C$ extends beyond R_C . However, in such a case Compton heating is sufficiently inefficient that the gas is in a time-dependent two-phase state. We do not consider this regime for ultraluminous quasars.

The radius of the Strömgen sphere of Fe^{26+} ions is given by

$$R_S^{\text{FeXXVI}} = \left(\frac{3\dot{N}_{\text{ion}}}{4\pi\alpha_{\text{Fe}}\mathcal{A}_{\text{Fe}}\mathcal{C}\langle n_b^2 \rangle} \right)^{1/3} = 5.7 L_{46}^{1/3} \mathcal{C}_4^{-1/3} \langle n_b^2 \rangle^{-1/3} \text{ kpc}, \quad (5)$$

where $\mathcal{C}_4 = \mathcal{C}/10^4$, $\alpha_{\text{Fe}} = 9.06 \times 10^{-12} \text{ cm}^3 \text{ s}^{-1}$ is the Fe^{26+} recombination coefficient in Seaton (1959) evaluated at $T_e = 3 \times 10^7 \text{ K}$, and $\langle n_b^2 \rangle_{-4} = \langle n_b^2 \rangle / 10^{-4} \text{ cm}^{-6}$ is the volume-averaged mean square density of the cold gas. The rate of ionizing photons, \dot{N}_{ion} , is estimated from the typical spectrum of quasars (Elvis et al. 1994). The radius of the He^{2+} Strömgen sphere $R_S^{\text{HeIII}} = 10.3 L_{46}^{1/3} \mathcal{C}_4^{-1/3} \langle n_b^2 \rangle^{-1/3} \text{ kpc}$, and $R_S^{\text{HeIII}}/R_S^{\text{HII}} \approx 0.3$; we assume ionization energies of $E_{\text{HeIII}} = 54.4 \text{ eV}$ and $E_{\text{HII}} = 13.6 \text{ eV}$ and an ionizing spectrum $f_\nu \propto \nu^{-1.3}$. The radius of the ionized region is given by (Cen & Haiman 2000) $R_{\text{ion}}^{\text{HeIII}} = (3\dot{N}_{\text{ion}}t_Q/4\pi\mathcal{A}_{\text{He}}\langle n_b^2 \rangle^{1/2})^{1/3} = 119 \tau_Q^{1/3} L_{46}^{1/3} \langle n_b^2 \rangle^{1/6} \text{ kpc}$, and $R_{\text{ion}}^{\text{HeIII}}/R_{\text{ion}}^{\text{HII}} = 1.2$. As the ionizing luminosity increases, the Compton radius extends to the radius of the helium Strömgen sphere. The entire Strömgen sphere will be fully heated to the Compton temperature when $R_S^{\text{FeXXVI}} = R_C$, at which point the iron Compton-limit luminosity

$$L_C^{\text{Fe}} = 3.0 \times 10^{47} \tau_Q^{-3} \mathcal{C}_4^{-2} \langle n_b^2 \rangle^{-2} \text{ erg s}^{-1}, \quad (6)$$

and the iron Compton-limit radius

$$R_C^{\text{Fe}} = 17.7 \tau_Q^{-1} \mathcal{C}_4^{-1} \langle n_b^2 \rangle^{-1} \text{ kpc}. \quad (7)$$

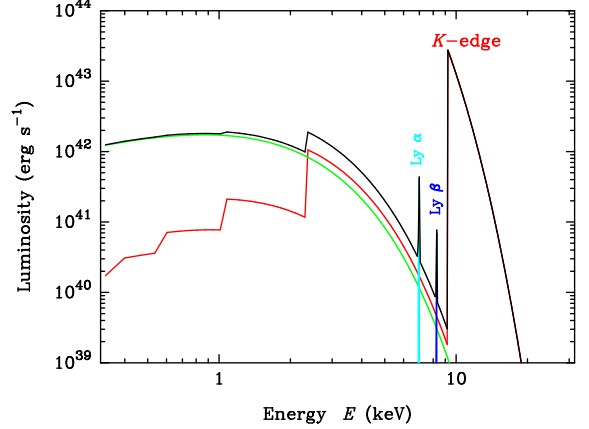


FIG. 2.— The X-ray spectrum of the Fe^{26+} Compton sphere. The green line represents free-free emission, the red line free-bound (radiative recombination) emission, and the black line the total emission from the Compton sphere. Iron $\text{Ly}\alpha$ $\lambda 1.78$ and $\text{Ly}\beta$ $\lambda 1.51$ lines, with emissivities (Raymond & Smith 1977) for $\sim 3 \times 10^7 \text{ K}$ and solar iron abundances, are labeled ($\Delta E/E = 0.02$ for *XEUS*). The $\text{Ly}\alpha$ and $\text{Ly}\beta$ lines will have equivalent widths of 12.0 keV and 6.6 keV for solar iron abundances, and should be detectable with *XEUS*.

When $L < L_C^{\text{Fe}}$, the Compton sphere is smaller than the Strömgen sphere. Since the medium in the region between the Strömgen radius and the Compton radius cannot fully reach the Compton temperature, the features of the afterglow arising from it could be complicated. We are currently interested in the case of $L \geq L_C^{\text{Fe}}$, namely, the ultraluminous quasars.

The energy stored within the Compton sphere, $\frac{4}{3}\pi R_C^3 n_e kT \approx 4 \times 10^{58} n_{-2} \text{ erg}$, where $T = 3.0 \times 10^7 \text{ K}$, $n_{-2} = n_e / 10^{-2} \text{ cm}^{-3}$, and $R_C = 20 \text{ kpc}$, is only a small fraction (0.02%) of the total energy released ($2 \times 10^{62} \text{ erg}$) during the activity of a quasar with a black hole mass of $10^9 M_\odot$ and an accretion efficiency of 0.1. The recombination timescale is $(\alpha_{\text{Fe}} n_e)^{-1} \approx 0.3 \times 10^7 n_{-2}^{-1} \text{ yr}$. For quasars surrounded by a very dilute medium, this timescale is too long for the ions to recombine within the Hubble time at the relevant epoch. The Strömgen radius is then never reached, and the hot gas would emit no recombination lines. This situation might be relevant for some isolated, exceptionally gas-poor elliptical galaxies. If the recombination timescale is longer than the lifetime of quasars, the discussion on the Strömgen radius is also inapplicable.

3. OBSERVATIONAL SIGNATURES

An afterglow will be seen from the Compton sphere after the quasar is extinct. Here we estimate the expected signature of the quasar afterglow from the hot gas inside the Compton sphere that is in hydrostatic equilibrium with the gravitational potential of the dark matter halo (Fig. 1). The isothermal density profile of the hot gas is given by (Makino et al. 1998) $\rho_g = \rho_0 e^{-\beta} (1 + R/R_s)^{\beta R_s/R}$, where $\rho_0 = 1.96 \times 10^{-26} \text{ g cm}^{-3}$, $\beta = 3.03 M_{13} T_7^{-1}$, the characteristic radius $R_s = 44.25 M_{13}^{1/3} \text{ kpc}$, $T_7 = T / 10^7 \text{ K}$, and $M_{13} = M_{\text{halo}} / 10^{13} M_\odot$. We use a concentration parameter of $c_0 = 5$ and $\Delta_c = 18\pi^2$ for the dark matter halo. The gas mass fraction is only $\sim 0.005 (\tau_{\text{es}} / 10^{-3})$ of that of the dark matter halo, where τ_{es} is the Thomson scattering depth of the hot gas. We note that the density of the hot gas is lower than the Compton density.

The cooling timescale of the fully ionized gas inside the Compton sphere is governed mainly by free-free radiation.

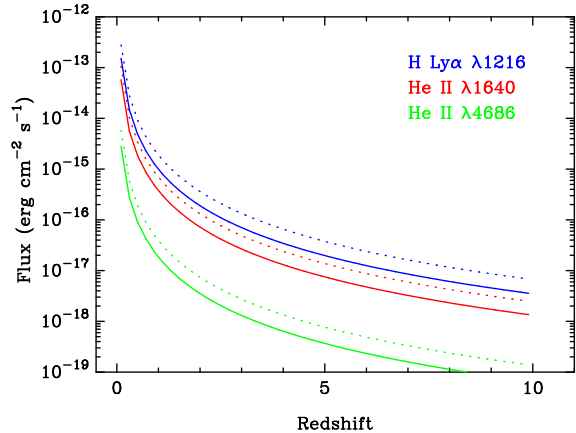


FIG. 3.— Expected fluxes of hydrogen ($\text{Ly}\alpha$ $\lambda 1216$) and helium (He II $\lambda\lambda 1640, 4686$) recombination lines. The solid and dotted lines show the predictions for an electron temperature of 10^4 K and 2×10^4 K, respectively. We assume a Λ CDM cosmology with $\Omega_m = 0.3$, $\Omega_\Lambda = 0.7$, and $H_0 = 75 \text{ km s}^{-1} \text{ Mpc}^{-1}$.

The cooling timescale at the center of the halo is $t_{\text{ff}} \approx 1.0 \times 10^9 T_7^{1/2} n_2^{-1} \text{ yr}$, and it will be considerably longer in the outskirts. This leads to the appearance of a long-lived, extended X-ray-emitting envelope, characterized by a luminosity $L_{\text{ff}} \approx 1.3 \times 10^{42} \text{ erg s}^{-1}$ for $T = 10^7$ K, $R_C = 20$ kpc and the above density profile, peaking at an energy of a few keV. Since the degree of ionization is very high during the active phase of the quasar, we assume that iron is fully ionized. Figure 2 shows the predicted X-ray signature from such a model, where we have computed the integrated emission from the Compton sphere of a progenitor quasar shining at a fiducial Compton luminosity of $10^{42} \text{ erg s}^{-1}$, including contributions from the K and L edges of Fe^{26+} free-bound emission from hydrogen-like ions (Seaton 1959) as well as the $\text{Ly}\alpha$ and $\text{Ly}\beta$ lines from Fe^{26+} . For redshifts $z \leq 0.2$, the expected flux of $\geq 1.1 \times 10^{-14} \text{ erg s}^{-1} \text{ cm}^{-2}$ will be detectable by *Chandra*/ACIS with an exposure time of 100 ks, and the angular radius of the Compton sphere, $\theta \approx 29.5''$, should be resolvable. However, the effective area of ACIS ($\sim 80 \text{ cm}^2$ above a few keV) is too small to be able to detect the $\text{Ly}\alpha$ and $\text{Ly}\beta$ lines of Fe^{26+} . The future *XEUS* mission, with an expected angular resolution of $2''$ at a flux level of $10^{-17} \text{ erg s}^{-1} \text{ cm}^{-2}$ in the energy range 0.05–30 keV, will be able to detect the Compton sphere and $\text{Ly}\alpha$ and $\text{Ly}\beta$ emission at redshifts lower than 1. Higher-redshift afterglows are too faint to be detected by *Chandra*, whereas *XEUS* will have insufficient resolution.

Lastly, we consider the signal from the region between the Compton radius and the ionization radius (Fig. 1), which arises from hydrogen and helium photoionized by the quasar. After the quasar quenches, the photoionized gas will radiate recombination lines of hydrogen and helium. We calculate the fluxes of hydrogen $\text{Ly}\alpha$ and He II $\lambda\lambda 1640, 4686$, using the recombination coefficients in Seaton (1978), by integrating the shell between the Compton and ionization radius (Fig. 3). The broadening width of the recombination lines due to thermal motions, $\Delta\lambda/\lambda \approx (kT_C/Zm_p c^2)^{1/2} \approx (0.2-3.0) \times 10^{-3}$, where Z is the charge of the ions. This width can be readily resolved by ground-based optical telescopes, the largest of which should also have the requisite sensitivity and spatial resolution to image the line-emitting region. We note that the emission-line regions considered here are different from the extended $\text{Ly}\alpha$

nebulae discovered in some star-forming galaxies (Steidel et al. 2000). The latter are powered by OB stars, which are not energetic enough to ionize He.

If quasar afterglows can be detected, either the luminosity or the size of the Compton sphere (Equations 6 and 7) can be used to estimate τ_Q , the lifetime of the progenitor quasar. In practice, the luminosity would be much better constrained than the size, as the latter would be only marginally resolved even with *Chandra* and depends critically on the detailed surface brightness distribution. While the hot gas normally associated with individual elliptical galaxies (O’Sullivan et al. 2003) rarely has temperatures exceeding 1 keV, galaxies situated in groups or denser environments would be surrounded by hotter gas, which at large distances would be difficult to distinguish from any component intrinsic to an afterglow. To minimize this source of confusion, the local environment of any potential targets needs to be carefully scrutinized. With typical X-ray temperatures of a few keV, X-ray binaries present another possible source of contamination, but their integrated X-ray emission (Fabbiano 1989), even in large galaxies, is significantly less than $10^{42} \text{ erg s}^{-1}$.

If quasars shine near the Eddington limit, the Compton-limit luminosity corresponds to a black hole mass $M_{\text{BH}} \approx 2 \times 10^9 M_\odot$. If such massive black holes are common among quasars (Netzer 2003; Vestergaard 2004), their afterglows should not be difficult to detect. From the $M_{\text{BH}} - \sigma$ relation (Tremaine et al. 2002), we expect the host galaxies to have stellar velocity dispersions of $\sigma \approx 400 \text{ km s}^{-1}$. Thus, future searches of quasar afterglows should target the most massive giant ellipticals. Such galaxies are rare, but not exceedingly so. From the local velocity dispersion function of early-type galaxies (Sheth et al. 2003), the space density of galaxies with $\sigma \approx 400 \text{ km s}^{-1}$ is $\sim 10^{-6} \text{ Mpc}^{-3}$.

For the more abundant but less powerful quasars, with luminosities below the Compton-limit luminosity, the Compton radius cannot match the Strömgren radius and it will be significantly smaller than the Compton-limit radius. The medium in the transition zone between the Compton and Strömgren radii is in a time-dependent two-phase state, since it is not able to reach an equilibrium state within the lifetime of the quasar. We speculate that these lower-luminosity sources would have optical and ultraviolet emission features quite similar to those of ultraluminous quasars, but that the X-ray spectrum should be dominated by the $\text{Ly}\alpha$ and $\text{Ly}\beta$ lines of lighter ions, such as Ne X or O VIII. Detailed calculations for this case are in progress.

4. SUMMARY

In conclusion, we show that the afterglows of ultraluminous quasars form relic Compton spheres that could be detected by *Chandra*, *XEUS*, and ground-based optical telescopes. The luminosities and sizes of the afterglows can be used to estimate the lifetime of quasars, a key constraint on quasar and galaxy evolution. The extended X-ray envelope recently detected around the isolated elliptical galaxy NGC 4555 (O’Sullivan & Ponman 2004) could be an example of the afterglows discussed in the present paper. It would be worthwhile to search in this object for the predicted extended emission from hydrogen and helium recombination lines.

We thank the referee, Dr. Markos Geoganopoulos, for helpful comments. This research is supported by a Grant for Distinguished Young Scientists through NSFC-10325303, NSFC-10222030 and 973 Projects. L.C.H. thanks the Carnegie Insti-

tution of Washington for support and J. S. Mulchaey for useful discussions.

REFERENCES

- Bergeron, J., et al. 1999, *A&A* 343, L40
Binney, J., & Tabor, G. 1995, *MNRAS*, 276, 663
Brighenti, F., & Mathews, W. G. 2002, *ApJ*, 573, 42
Bunker, A. J., Smith, J., Spinrad, H., Stern, D., & Warren, S. 2003, *ApS&S*, 284, 357
Cen, R., & Haiman, Z. 2000, *ApJ*, 542, L75
Ciotti, L. D., & Ostriker, J. P. 2001, *ApJ*, 551, 131
Elvis, M., et al. 1994, *ApJS*, 95, 1
Fabbiano, G. 1989, *AR&AA*, 27, 87
Fall, S. M., & Rees, M. J. 1985, *ApJ*, 298, 18
Fardal, M. A., et al. 2001, *ApJ*, 562, 605
Haiman, Z., & Rees, M. J. 2001, *ApJ*, 556, 87
Haiman, Z., Spaans, M., & Quataert, E. 2000, *ApJ*, 537, L5
Jakobsen, P., Jansen, R. A., Wagner, S., & Reimers, D. 2003, *A&A*, 397, 891
Krolik, J. H., McKee, C. F., & Tarter, C. B. 1981, *ApJ*, 249, 422
Makino, N., et al. 1998, *ApJ*, 497, 555
Martini, P., & Schneider, D. P. 2000, *ApJ*, 597, L109
Mathews, W. G., & Brighenti, F. 2003, *ARA&A*, 41, 191
Netzer, H. 2003, *ApJ*, 583, L5
O'Sullivan, E., & Ponman, T. J. 2004, *MNRAS*, 354, 935
O'Sullivan, E., Ponman, T. J., & Collins, R. S. 2003, *MNRAS*, 340, 1375
Raymond, J. C., & Smith, B. W. 1977, *ApJ*, 35, 419
Salpeter, E. E. 1964, *ApJ*, 140, 796
Sazonov, S. Yu, Ostriker, J. P., & Sunyaev, R. A. 2004, *MNRAS*, 347, 144
Seaton, M. J. 1959, *MNRAS*, 119, 81
———. 1978, *MNRAS*, 185, 5P
Sheth, R. K., et al. 2003, *ApJ*, 594, 225
Steidel, C. C., et al. 2000, *ApJ*, 532, 170
Tremaine, S., et al. 2002, *ApJ*, 574, 740
Vestergaard, M. 2004, *ApJ*, 601, 676
Weidinger, M., Møller, P., & Fynbo, J. P. U. 2004, *Nature*, 430, 999